

Granular-composite-like electrical transport properties of polycrystalline cubic TaN_x thin films prepared by rf sputtering method

Ran Li,¹ Xiu-Zhi Duan,¹ Xin Zhu,¹ Yang Yang,¹ Ding-Bang Zhou,² and Zhi-Qing Li^{1,*}

¹*Tianjin Key Laboratory of Low Dimensional Materials Physics and Preparing Technology,
Department of Physics, Tianjin University, Tianjin 300354, China*

²*Tianjin University Analysis Centre, Tianjin University, Tianjin 300072, China*
(Dated: April 7, 2024)

We have systematically investigated the electrical transport properties of polycrystalline TaN_x ($0.83 \lesssim x \lesssim 1.32$) films with rocksalt structure from 300 down to 2 K. It is found that the conductivity varies linearly with $\ln T$ from ~ 6 K to ~ 30 K, which does not originate from the conventional two dimensional weak-localization or electron-electron interaction effects, but can be well explained by the intergrain Coulomb effect which was theoretically proposed in the granular metals. While the fluctuation-induced tunneling conduction process dominates the temperature behaviors of the conductivities (resistivities) above ~ 60 K. Normal state to superconductive state transition is observed in the $x \gtrsim 1.04$ films in low temperature regime. The superconductivity can still be retained at a field of 9 T. The upper critical field increases linearly with decreasing temperature in the vicinity of the superconductive transition temperature, which is the typical feature of granular superconductors or dirty type-II superconductors. The granular-composite-like electrical transport properties of the polycrystalline TaN_x films are related to their microstructure, in which the TaN_x grains with high conductivity are separated by the poorly conductive amorphous transition layers (grain boundaries).

Keywords: Transition metal nitride, Transport properties, Granular composites

I. INTRODUCTION

During the last decades, tantalum nitride (TaN_x) with rocksalt structure has received much attention due to its high hardness [1], good wear resistance [2], chemical inertness [3], thermodynamic stability [4], and low temperature coefficients of resistivity [5]. Besides these excellent properties, the TaN_x in rocksalt structure possesses superconductivity at liquid helium temperatures and has a small superconducting energy gap, thus it is potential candidate material for superconducting nanowire single-photon detectors [6]. In addition, the resistivity of the rocksalt TaN_x can be as low as $\sim 2 \times 10^{-4} \Omega \text{ cm}$, which makes TaN_x be good exemplary material for investigating the abundant physics near superconductor-insulator transition [7–9]. Although the TaN_x films have been technologically applied in many fields, some fundamental issues are still not clear. For example, the density-functional theory (DFT) calculation results indicate that TaN_x in the rocksalt structure has a metallic nature in energy-band structure [10, 11]. However, numerous experimental results show TaN_x in the rocksalt structure has negative temperature coefficient of resistivity (TCR, here TCR is defined as $d\rho/(\rho dT)$, and ρ is the resistivity at a certain temperature T) [5, 12], and the origins of the negative TCR is still debatable. Tiwari *et al* ascribed the negative TCR of TaN films to weak-localization effect [13], while the hopping conduction and electron-electron (e - e) interaction effect were considered as the origins by other groups [14, 15]. Thus further investigations on the fundamental properties, especially

with regard to the electrical transport properties, are still needed for the TaN_x compounds. In the present paper, we investigate the electrical transport properties of rocksalt TaN_x thin films with $0.8 \lesssim x \lesssim 1.3$. The cross-section high resolution electron transmission microscopy images and transport results indicate the TaN_x thin films are similar to the ‘conductor-insulator granular composites’ in morphologies and electrical transport properties, respectively. In additions, it is found that a field of up to 9 T cannot destroy the superconductivity of the TaN_x films with $x \gtrsim 1.04$. We report our results in the following discussions.

II. EXPERIMENTAL METHOD

The samples were deposited on quartz glass substrates by rf sputtering method. The size of the substrate is $5 \text{ mm} \times 10 \text{ mm}$. Considering Ta-N compounds can exhibit a variety of crystallographic phases such as cubic, hexagonal, and tetragonal, we chose a commercial TaN target, in which the nominal atomic ratio of Ta to N is ~ 1 (provided by Shanghai Institute of Optics and Fine Mechanics, Chinese Academic of Science), as the sputtering source to avoid producing impure phases. Indeed, it is found that the rocksalt structure single phase TaN_x film can be readily obtained only in Ar atmosphere. The chamber was pre-pumped down to $9 \times 10^{-5} \text{ Pa}$ and the argon (99.999% in purity) pressure was maintained at 0.6 Pa during sputtering. The substrate temperature was set as 873 K and the composition of the films was tuned by changing the sputtering power from 70 W to 130 W. We also deposited an amorphous film at room temperature for comparison (sputtering power 130 W). The thicknesses of the films,

* Corresponding author, e-mail: zhiqingli@tju.edu.cn

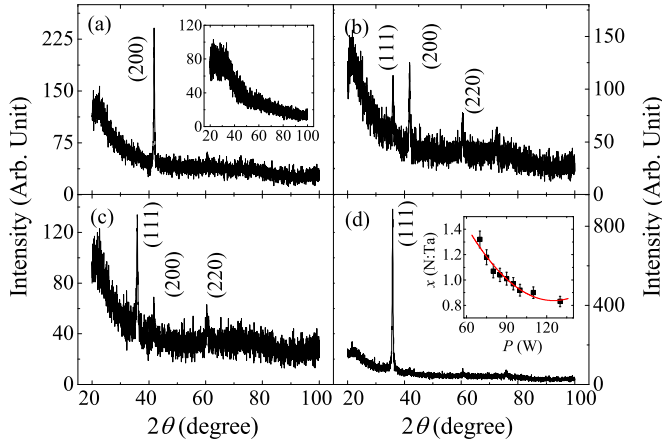


FIG. 1. XRD diffraction patterns for the TaN_x deposited at different sputtering powers, (a) 70 W, (b) 80 W, (c) 90 W, and (d) 100 W, the substrate temperatures for all the films are 873 K. The inset in (a) is the XRD diffraction pattern of Ta-N films deposited at room temperature and 130 W. The inset in (d) presents the ratio of N to Ta, x , versus sputtering power P . The solid curve in the inset of (d) is only guide to eyes.

~ 150 nm, were measured with a surface profiler (Dektak, 6 M). The crystal structures of the films were measured using a x-ray diffractometer (XRD, D/MAX-2500v/pc, Rigaku) with $\text{Cu K}\alpha$ radiation. The composition of the films was obtained from the energy-dispersive x-ray spectroscopy analysis (EDS). The microstructure of the films was characterized by transmission electron microscopy (TEM, Tecnai G2 F20). The resistivities and Hall effect measurements were carried out in a physical property measurement system (PPMS-6000, Quantum Design) by employing the standard four-probe methods. Hall-Bar-shaped films (1 mm wide, 10 mm long, and the distance between the two voltage electrodes is 3.6 mm) defined by mechanical masks were used for the measurements. For the amorphous film with high resistance, a Keithley 6221 current source and a Keithley 2182A nanovoltmeter were used in the four-probe configuration.

III. RESULTS AND DISCUSSIONS

Figure 1 shows the XRD patterns of films deposited at 873 K but different sputtering powers. The inset of Fig. 1 (a) is the diffraction pattern for film deposited at room temperature. There is no sharp peak appear in the pattern, indicating the film is amorphous. When the substrate temperature is enhanced to 873 K, relatively weak diffraction peaks appear. For each film, the diffraction peaks can be indexed based on the face centered cubic structure (rocksalt structure) TaN (PDF No.49-1283), and other phases, such as, hexagonal or tetragonal structure Ta-N compounds are not detected. For the film de-

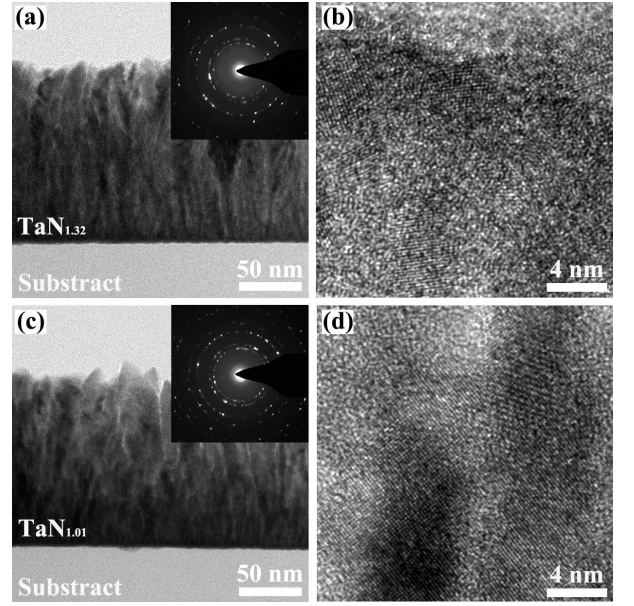


FIG. 2. Cross-sectional TEM images of two representative films, (a) and (b) for $\text{TaN}_{1.32}$ film, and (c) and (d) for $\text{TaN}_{1.01}$ film. Figures (b) and (d) are high-resolution images. The insets are the SAED patterns for the corresponding films.

posited at 70 W, the preferred growth orientation is along [200] direction. Along with increasing sputtering power, the relative intensity of (111) peak gradually increases while the relative intensity of (200) decreases. When the sputtering power is enhanced to ~ 100 W, the intensity of (111) peak is far greater than that of the diffractions of other planes, i.e., the (111) direction becomes the preferred growth orientation. The inset of Fig. 1 (d) shows the ratio of N to Ta, x , varies as a function of sputtering power. The x value decreases monotonously with increasing sputtering power. The maximum and minimum values of x are 1.32 and 0.83, respectively. Our results indicate that TaN_x films could maintain the rocksalt structure in the regime $0.8 \lesssim x \lesssim 1.3$, which is consistent with the results of other groups [1, 12, 16]. Considering the composition is one of the key elements determining the intrinsic properties of materials, we use TaN_x instead of sputtering power to identify our films in the following discussions.

Figure 2 shows the cross-sectional TEM images and selected-area diffraction patterns (insets) of $\text{TaN}_{1.32}$ and $\text{TaN}_{1.01}$ films. From Fig. 2 (a) and (c), one can see that the compact films reveal columnar growth features. From the cross-section images, we can obtain the average thickness of the films, which is identical to that measured in the surface profiler. Figure 2 (b) and (d) present the high resolution TEM images of the films. Inspection of the high resolution TEM images indicates that the mean grain sizes are ~ 5 nm and the TaN_x grains are separated by amorphous boundaries with thickness ~ 2 to ~ 3 nm for both films. We note in passing that the selected area

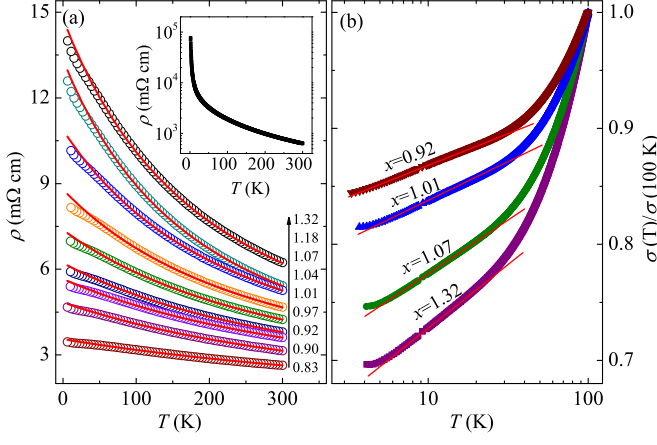


FIG. 3. (a) Resistivities versus temperature from 5 to 300 K for the polycrystalline TaN_x films. (b) Normalized conductivities versus temperature from 4 to 100 K. The solid curves in (a) and (b) are least-squares fits to Eq. (2) and Eq. (1), respectively. The inset in (a) is the variation in the logarithm of resistivity with temperature from 300 down to 2 K for the amorphous $\text{TaN}_{0.87}$ film.

electron diffraction (SAED) patterns (insets in Fig. 2) also reveal a pure rocksalt structure of the films.

Figure 3 (a) shows the temperature dependence of resistivity for the polycrystalline TaN_x films with different x , as indicated. The resistivity increases monotonically with decreasing temperature from 300 down to 5 K for each film. At a certain temperature, the resistivity decreases with decreasing x . For the TaN_x films, larger x could lead to higher concentration of Ta vacancy (V_{Ta}). Yu *et al* have calculated the electronic structure of non-stoichiometric TaN_x with rocksalt structure [16]. Their results indicate that with increasing V_{Ta} concentration, the electron density of states (DOS) at Fermi level diminishes monotonically, corresponding to a reduction in the free carrier concentration. V_{Ta} therefore spatially localizes free carriers in the conduction band. The Hall effect measurements indicate that the main charge carrier in the TaN_x film is electron and carrier concentration decreases with increasing x (see Table I). Thus the reduction of resistivity with decreasing x in our TaN_x films can be partially attributed to the reduction of the concentration of V_{Ta} with reducing x .

Since the polycrystalline TaN_x films are composed of TaN_x grains separated by amorphous TaN_x transition layers (the grain boundaries), we review the conduction behavior of the amorphous Ta-N film before analyzing the transport properties of the polycrystalline films. The EDS result indicates that the atomic ratio of N to Ta in the amorphous film is ~ 0.87 , which is almost identical to that of the polycrystalline one deposited at 873 K (substrate temperature) and the same sputtering power (130 W) within the experimental uncertainty ($\sim 5\%$). The inset of Fig. 3 (a) shows the variation in the

logarithm of resistivity with temperature from 300 down to 2 K for the amorphous $\text{TaN}_{0.87}$ film. The resistivity increases with decreasing temperature over the whole measured temperature range, and the enhancement of the resistivity is larger than 2 orders of magnitude as the temperature decreases from 300 to 2 K. At a certain temperature, the resistivity of the amorphous $\text{TaN}_{0.87}$ film is much greater than that of the polycrystalline one. For example, the resistivity of the amorphous $\text{TaN}_{0.87}$ film is ~ 2 (4) orders of magnitude larger than that of the polycrystalline $\text{TaN}_{0.83}$ or $\text{TaN}_{0.90}$ films at 300 K (5 K). Considering the resistivity of the grain boundaries in the polycrystalline TaN_x film is far larger than that of the grains, one expects that the transport properties of the polycrystalline TaN_x films would be similar to that of the ‘conductor-insulator’ granular composite.

Recently, the electrical transport properties of ‘conductor-insulator’ granular composite have been intensively investigated both in theoretical [17–19] and experimental [20, 27–29] sides. It has been found that in the strong coupling limit and in high energy regime ($k_B T > g_T \delta$, where g_T is dimensionless conductance, $g_T = G_T / (2e^2 / \hbar)$, G_T is the average tunneling conductance between neighboring grains, e is the elementary charge, \hbar is the Planck’s constant divided by 2π , δ is the mean level spacing in a single grain, k_B is the Boltzmann constant), the temperature behavior of the conductivity (not the resistivity) of the granular composites is governed by the intergrain Coulomb effects and the conductivity can be written as [17–19]

$$\sigma = \sigma_0 \left[1 - \frac{1}{2\pi g_T d} \ln \left(\frac{g_T E_c}{k_B T} \right) \right] \quad (1)$$

in the temperature interval $g_T \delta < k_B T < E_c$, where σ_0 is the classical conductivity without the intergrain Coulomb effects, E_c is the charging energy of an isolated grain, d is the dimensionality of the granular array. It should be noted that the logarithmic behavior of the conductivity in Eq. (1) is specific to granular system and physically distinct from that predicted by the conventional two dimensional (2D) weak-localization and electron-electron (e - e) interaction effects in homogeneous disordered conductors [21–25].

Figure 3 (b) presents the temperature dependence of the normalized conductivity from 4 to 100 K. In the measurement process, a magnetic field of 9 T perpendicular to the film plane was applied to suppress the weak-localization (antilocalization) [21, 22], and superconducting fluctuation effects [26]. Clearly, the conductivity varies linearly with $\log T$ (or $\ln T$) from ~ 6 to ~ 30 K for each film. The solid straight lines in Fig. 3 (b) are the least-squares fits to Eq.(1) with $d=3$. In the fitting processes, σ_0 and g_T were treated as adjusting parameters, and the upper bound temperature E_c/k_B for Eq.(1) to hold was taken as $\simeq 40$ K. The obtained values of σ_0 and g_T are listed in Table I. Inspection of Table I indicates the value of g_T varies from 0.80 to 3.70, which satisfy the condition $g_T > g_T^c$, where $g_T^c = (1/2\pi d) \ln(E_c/\delta)$ is the critical

TABLE I. Relevant parameters for the polycrystalline TaN_x films. Here x is the atomic ratio of N to Ta, t is the thickness of the film, n is the carrier (electron) concentration, g_T is dimensionless conductance, ρ_1 , T_1 , and T_0 are parameters in Eq. (2), and ξ_0 is the zero-temperature clean limit coherence length.

x	t (nm)	$\rho(300\text{ K})$ (m Ω cm)	$n(200\text{ K})$ (10 ²¹ cm ⁻³)	σ_0 (S/m)	g_T	ρ_1 (m Ω cm)	T_1 (K)	T_0 (K)	T_0/T_1	T_1^2/T_0 (10 ³ K)	ξ_0 (nm)
1.32	150	6.23	0.59	7762	0.80	1.33	1292	536	0.414	3.11	2.20
1.18	155	5.42	0.75	8673	0.85	1.20	1208	502	0.415	2.91	2.23
1.07	153	5.26	1.49	10425	1.09	1.18	1364	616	0.452	3.02	2.38
1.04	155	4.67	3.66	12981	1.67	1.14	1365	667	0.489	2.79	2.87
1.01	145	4.24	5.44	15118	1.69	0.99	1575	785	0.499	3.16	-
0.97	150	3.80	5.71	17742	1.86	0.91	1676	872	0.520	3.22	-
0.92	150	3.61	11.11	19343	2.04	0.89	1704	925	0.543	3.14	-
0.90	152	3.15	18.60	22536	2.36	0.81	1671	934	0.559	2.99	-
0.83	160	2.64	21.46	30228	3.70	0.74	1988	1259	0.633	3.14	-

tunneling conductance for metal-insulator transition and about 0.1 for the TaN_x films. Hence our experimental data in the temperature range 6 to ~ 30 K can be well described by Eq.(1). It is well known that the conventional e - e interaction effects could also lead to a small $\ln T$ correction to the conductivity in 2D homogeneous disordered system. The characteristic length concerning the dimensionality of interaction effect is the electron diffusion length $L_T = \sqrt{\hbar D/k_B T}$, where D is the electron diffusion constant. For our TaN_x films, the maximum value of L_T at 10 K is ≈ 9 nm (the $x \approx 0.83$ film), which is much less than the thickness of the film (~ 150 nm). Thus our TaN_x films are 3D with regard to e - e interaction effect. Since the correction to conductivity due to 3D e - e interaction effect is proportional to \sqrt{T} , the $\ln T$ behavior of the conductivity in the TaN_x films in low temperature regime can be safely ascribed to the Coulomb effects in the presence of granularity.

At $T > E_c/k_B$, the thermally activated voltage fluctuation across the insulator region would play important role in the temperature dependence of the resistivity of ‘conductor-insulator’ or ‘conductor-semiconductor’ granular composite. This is the fluctuation-induced tunneling (FIT) conduction process [30–33]. According to Sheng *et al* [30, 31], the FIT resistivity can be express as

$$\rho = \rho_1 \exp\left(\frac{T_1}{T + T_0}\right), \quad (2)$$

where ρ_1 is prefactor which only weakly depends on temperature, and T_1 and T_0 are parameters related to the barrier and defined as [30–33]

$$T_1 = \frac{8\epsilon_0\epsilon_r AV_0^2}{e^2 k_B w}, \quad (3)$$

and

$$T_0 = \frac{16\epsilon_0\epsilon_r \hbar AV_0^{3/2}}{\pi(2m)^{1/2} e^2 k_B w^2}. \quad (4)$$

Here ϵ_0 is the permittivity of vacuum, ϵ_r is the relative permittivity, A is the barrier area, V_0 is the bar-

rier height, w is the barrier width, and m is the mass of charge carrier. The $\rho(T)$ data of the TaN_x films are least-squares fitted to Eq. (2) and the results are shown as solid curves in Fig. 3 (a). The fitting parameters T_1 and T_0 for each film are listed in Table I. Clearly, the predication of Eq. (2) can well reproduce the experimental data from ~ 60 to 300 K. Due to lacking the data of relative permittivity of amorphous TaN_x compound, we qualitatively discuss the fitting results here. From Eq. (3) and Eq. (4), one can obtain,

$$\frac{T_0}{T_1} = \frac{2}{\pi \chi w}, \quad (5)$$

and

$$\frac{T_1^2}{T_0} = \frac{4\pi A \epsilon_0 \epsilon_r V_0^2 \chi}{k_B e^2} \propto A V_0^{5/2}, \quad (6)$$

where $\chi = (2mV_0/\hbar^2)^{1/2}$. The values of T_0/T_1 and T_1^2/T_0 are also listed in Table I. The values of T_1^2/T_0 are close to ~ 3000 K for all films while the values of T_0/T_1 increase with decreasing x . Neglecting the difference of the barrier area (A) between different films, one can obtain that the variation of barrier hight V_0 between different films can be ignored. Thus, with the decrease of x , the slight enhancement of T_0/T_1 means the slight reduction of the barrier width w , which is consistent with the enhancement of g_T mentioned above.

Figure 4 (a) shows the normalized resistivity $\rho/\rho(5\text{ K})$ as a function of temperature from 5 down to 2 K for the polycrystalline TaN_x films. Here 2 K is the minimum temperature that could be reached in our PPMS system (⁴He system). For films with $x \gtrsim 1.04$, the resistivities decrease to zero above 2 K. We designate the critical temperature T_c as the temperature at which the resistivity has dropped to $\rho_N/2$, where the normal state resistivity ρ_N is taken as the value at 5 K. While for films with $x \lesssim 1.01$, the resistivities also drop sharply with decreasing temperature, but do not reach to zero within the resolution limit of our instrument ($\sim 10^{-4} \Omega$). Ac-

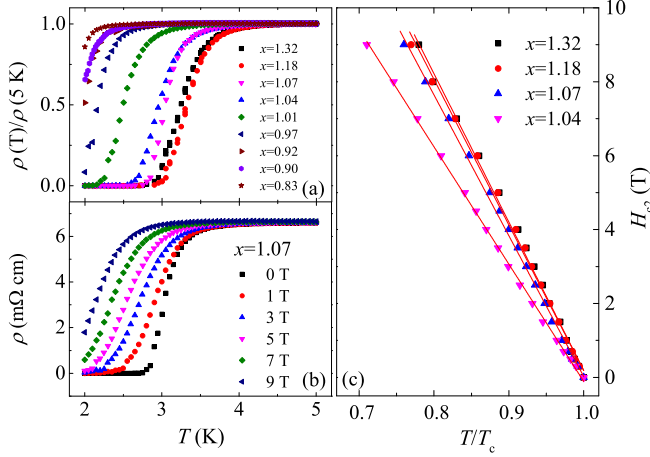


FIG. 4. (a) Normalized resistivities versus temperature for the polycrystalline TaN_x films. (b) Resistivity as a function of temperature under perpendicular magnetic fields from 0 to 9 T for $\text{TaN}_{1.07}$ film. (c) Perpendicular upper critical field as a function of temperature for TaN_x films with $x \approx 1.32, 1.18, 1.07$, and 1.04 .

cording to Shin *et al* [1], the superconducting transition temperature T_c of the epitaxial rocksalt structure TaN_x film with $x \sim 1$ is ~ 8 K, which is much greater than that in our films. Recently, it was reported that the superconducting transition temperature can be seriously suppressed by the granular effect in superconductor with small energy gap. For example, the reduction of the transition temperature in Nb polycrystalline film had been ascribed to the presence of Nb_2O_5 between the neighboring Nb grains. The smaller the Nb grain size, the lower transition temperature the Nb film has [34, 35]. Thus the lower superconducting transition temperature of the polycrystalline TaN_x films could be result from ‘conductor-insulator’ granular nature of the films.

Figure 4 (b) shows the temperature dependence of the resistivity under different magnetic fields for the $x \approx 1.07$ film. Clearly, the normal state is still not restored in field as large as 9 T (the maximum field could be reached in our PPMS system). Designating the upper critical field as the field at which the resistivity has dropped to $\rho_N/2$, we obtain the H_{c2} as a function of the normalized temperature T/T_c for the $x \gtrsim 1$ films and show them in Fig. 4 (c). The upper critical fields almost increase linearly with decreasing temperature and have already reached 9 T at $T \sim 0.75T_c$, which is much greater than that of the reported ones [8, 36, 37]. It was well established that the granular superconductor composite behavior as a dirty type-II material and its upper critical field is appreciably higher than that of the single component bulk material [38, 39]. Thus the large upper critical field in our polycrystalline TaN_x films mainly arises from the ‘conductor-insulator’ characteristics of the films.

According to Deutscher *et al* [38], in the strong cou-

pling limit and weak-field case, the temperature behavior of the upper critical field is similar to that of a dirty type-II superconductor,

$$H_{c2}(T) = \frac{\Phi_0}{2\pi\xi^2(T)}, \quad (7)$$

where $\Phi_0 = h/2e$ is the flux quantum and $\xi(T)$ is the Ginzburg-Landau coherence length. In the vicinity of T_c , the coherence length $\xi(T)$ is given by [40–42]

$$\xi(T) = 0.85 \left(\xi_0 l \frac{T_c}{T_c - T} \right)^{1/2}, \quad (8)$$

where l is the electronic mean free path, ξ_0 is the zero-temperature clean limit coherence length. For the $x \gtrsim 1$ TaN_x films, we take the value of l as the mean grain size (~ 5 nm) and compare the theoretical predication of Eq. (7) with our experimental data. The value of the adjustable parameter ξ_0 is listed in Table I, and slightly less than the mean grain size for each film. Inspection Fig. 4 (c) indicates that the experimental $H_{c2}(T)$ data in the vicinity of T_c can be well described by Eq. (7), which in turn demonstrates the temperature behaviors of H_{c2} in the polycrystalline TaN_x films are also similar to that of ‘superconductor-insulator’ granular composites.

IV. CONCLUSION

In summary, we have fabricated a series of polycrystalline TaN_x ($0.83 \lesssim x \lesssim 1.32$) films with rocksalt structure using a TaN target by rf sputtering method. High-resolution TEM measurements indicate the films are composed of TaN_x grains with amorphous grain boundaries. It is found that the resistivity of amorphous TaN_x film is far greater than that of the polycrystalline one. The conductivities of the polycrystalline TaN_x vary linearly with $\ln T$ from ~ 6 to ~ 30 K, which is explained as originating from the intergrain Coulomb interaction effect in the presence of granularity as theoretically predicted. Above ~ 60 K, the thermal activated voltage fluctuation across insulating region governs the temperature behaviors of the resistivities (conductivities). Superconductive transition is observed in the $x \gtrsim 1.04$ films and their upper critical fields are greater than 9 T. In the vicinity of the superconductive transition temperature, the upper critical field increases linearly with decreasing temperature, which is the typical feature of granular superconductors or dirty type-II superconductors. These granular-composite-like transport properties are ascribed to the ‘conductor-insulator’-like microstructure of the TaN_x films.

ACKNOWLEDGMENTS

This work is supported by the National Natural Science Foundation of China (Grant No. 11774253).

-
- [1] C.S. Shin, D. Gall, Y.W. Kim, P. Desjardins, I. Petrov, J.E. Greene, Epitaxial NaCl structure δ -TaN_x(001): Electronic transport properties, elastic modulus, and hardness versus N/Ta ratio, *J. Appl. Phys.* 90 (2001) 2789-2885.
 - [2] K. Baba, R. Hatada, Synthesis and properties of tantalum nitride films formed by ion beam assisted deposition, *Surf. Coat. Technol.* 84 (1996) 429-433.
 - [3] E. Kolawa, J.S. Chen, J.S. Reid, P.J. Pokela, M.A. Nicolet, Tantalum-based diffusion barriers in Si/Cu VLSI metallizations, *J. Appl. Phys.* 70 (1991) 1369-1373.
 - [4] M. Lane, R.H. Dauskardt, N. Krishna, I. Hashim, Adhesion and reliability of copper interconnects with Ta and TaN barrier layers, *J. Mater. Res.* 15 (2000) 203-211.
 - [5] N.D. Cuong, N.M. Phuong, D.J. Kim, B.D. Kang, C.S. Kim, S.G. Yoon, Effect of annealing temperature on structural and electrical properties of tantalum nitride thin film resistors deposited on SiO₂/Si substrates by dc sputtering technique, *J. Vac. Sci. Technol B* 24 (2006) 682-685.
 - [6] A. Engel, A. Aeschbacher, K. Inderbitzin, A. Schilling, K. Ilin, M. Hofherr, M. Siegel, A. Semenov, H.W. Hübers, Tantalum nitride superconducting single-photon detectors with low cut-off energy, *Appl. Phys. Lett.* 100 (2012) 062601.
 - [7] S. Chaudhuri, I.J. Maasilta, Superconducting tantalum nitride-based normal metal-insulator-superconductor tunnel junctions, *Appl. Phys. Lett.* 104 (2014) 122601.
 - [8] N.P. Breznay, M. Tendulkar, L. Zhang, S.C. Lee, A. Kapitulnik, Superconductor to weak-insulator transitions in disordered tantalum nitride films, *Phys. Rev. B* 96 (2017) 134522.
 - [9] N.P. Breznay, A. Kapitulnik, Particle-hole symmetry reveals failed superconductivity in the metallic phase of two-dimensional superconducting films, *Sci. Adv.* 3 (2017) e1700612.
 - [10] T.E. Kim, S. Hana, W. Son, E. Cho, H.S. Ahn, S. Shin, Phase stability and electronic structures of stoichiometric tantalum mononitrides, *Comput. Mater. Sci.* 44 (2008) 577-580.
 - [11] C.L. Cao, Z.F. Hou, G. Yuan, First-principles study of the structural stability and electronic structures of TaN, *Phys. Status Solidi B* 245 (2008) 1580-1585.
 - [12] C.S. Shin, D. Gall, P. Desjardins, A. Vailionis, H. Kim, I. Petrov, J.E. Greene, Growth and physical properties of epitaxial metastable cubic TaN(001), *Appl. Phys. Lett.* 75 (1999) 3808-3810.
 - [13] A. Tiwari, H. Wang, D. Kumar, J. Naryan, Weak-localization effect in single crystal TaN(001) films, *Mod. Phys. Lett. B* 16 (2002) 1143-1149.
 - [14] K. Lala, P. Ghosha, D. Biswasa, A.K. Meikap, S.K. Chattopadhyaya, S.K. Chatterjee, M. Ghosh, K. Babac, R. Hatadac, A low temperature study of electron transport properties of tantalum nitride thin films prepared by ion beam assisted deposition, *Solid State Commun.* 131 (2004) 479-484.
 - [15] M. Očko, S. Žonja, G.L. Nelson, J.K. Freericks, L. Yu, N. Newman, Low-temperature transport properties of Ta_xN thin films ($0.72 \leq x \leq 0.83$), *J. Phys. D: Appl. Phys.* 43 (2010) 445405.
 - [16] L. Yu, C. Stampfl, D. Marshall, T. Eshrich, V. Narayanan, J.M. Rowell, N. Newman, A.J. Freeman, Mechanism and control of the metal-to-insulator transition in rocksalt tantalum nitride, *Phys. Rev. B* 65 (2002) 245110.
 - [17] I.S. Beloborodov, A.V. Lopatin, V.M. Vinokur, K.B. Efetov, Granular electronic systems, *Rev. Mod. Phys.* 79 (2) (2007) 469.
 - [18] I.S. Beloborodov, K.B. Efetov, A.V. Lopatin, V.M. Vinokur, Transport properties of granular metals at low temperatures, *Phys. Rev. Lett.* 91 (2003) 246801.
 - [19] K.B. Efetov, A. Tschersich, Coulomb effects in granular materials at not very low temperatures, *Phys. Rev. B* 67 (2003) 174205.
 - [20] R. Sachser, F. Porrati, C.H. Schwalb, M. Huth, Universal conductance correction in a tunable strongly coupled nanogranular metal, *Phys. Rev. Lett.* 107 (2011) 206803.
 - [21] P.A. Lee, T.V. Ramakrishnan, Disordered electronic systems, *Rev. Mod. Phys.* 57 (1985) 287.
 - [22] G. Bergmann, Weak localization in thin films, *Phys. Rep.* 107 (1984) 1.
 - [23] B.L. Altshuler, A.G. Aronov, P.A. Lee, Interaction effects in disordered Fermi systems in two Dimensions, *Phys. Rev. Lett.* 44 (1980) 1288.
 - [24] B.L. Altshuler, D. Khmel'nitzkii, A.I. Larkin, P.A. Lee, Magnetoresistance and Hall effect in a disordered two-dimensional electron gas, *Phys. Rev. B* 22 (1980) 5142.
 - [25] J.J. Lin, J.P. Bird, Recent experimental studies of electron dephasing in metal and semiconductor mesoscopic structures, *J. Phys.: Condens. Matter* 14 (2002) R501.
 - [26] A. Gerber, A. Milner, G. Deutscher, M. Karpovsky, A. Gladkikh, Insulator-superconductor transition in 3D granular Al-Ge films, *Phys. Rev. Lett.* 78 (1997) 4277.
 - [27] Y.C. Sun, S.S. Yeh, J.J. Lin, Conductivity and tunneling density of states in granular Cr films, *Phys. Rev. B* 82 (2010) 054203.
 - [28] Y.J. Zhang, Z.Q. Li, J.J. Lin, Logarithmic temperature dependence of Hall transport in granular metals, *Phys. Rev. B* 84 (2011) 052202.
 - [29] Y.N. Wu, Y.F. Wei, Z.Q. Li, Electron-electron interaction effect on longitudinal and Hall transport in thin and thick Ag_x(SnO₂)_{1-x} granular metals, *Phys. Rev. B* 91 (2015) 104201.
 - [30] P. Sheng, E.K. Sichel, J.I. Gittleman, Fluctuation-induced tunneling conduction in carbon-polyvinylchloride composites, *Phys. Rev. Lett.* 40 (1978) 1197.
 - [31] P. Sheng, Fluctuation-induced tunneling conduction in disordered materials, *Phys. Rev. B* 21 (1980) 2180.
 - [32] Y.H. Lin, S.P. Chiu, J.J. Lin, Thermal fluctuation-induced tunneling conduction through metal nanowire contacts, *Nature Nanotech.* 19 (2008) 365201.
 - [33] X.D. Liu, J. Liu, S. Chen, Z.Q. Li, Electrical transport properties of Al-doped ZnO films, *Appl. Surf. Sci.* 263 (2012) 486.
 - [34] S. Bose, P. Raychaudhuri, R. Banerjee, P. Vasa, P. Ayyub, Mechanism of the size dependence of the superconducting transition of nanostructured Nb, *Phys. Rev. Lett.* 95 (2005) 147003.
 - [35] S. Bose, R. Banerjee, A. Genc, P. Raychaudhuri, H.L. Fraser, P. Ayyub, Size induced metal-insulator transition

- in nanostructured niobium thin films: intra-granular and inter-granular contributions, *J. Phys.: Condens. Matter* 18 (2006) 4553-4566.
- [36] N.P. Breznay, K. Michaeli, K.S. Tikhonov, A.M. Finkelstein, M. Tendulkar, A. Kapitulnik, Hall conductivity dominated by fluctuations near the superconducting transition in disordered thin films, *Phys. Rev. B* 86 (2012) 014514.
- [37] K.S. Ilin, D. Rall, M. Siegel, A. Semenov, Critical current density in thin superconducting TaN film structures, *Physica C* 479 (2012) 176-178.
- [38] G. Deutscher, O.E. Wohlman, Y. Shapira, Upper critical fields in granular superconductors, *Phys. Rev. B* 22 (1980) 4264.
- [39] S.Y. Hsu, J.M.V. Jr, Perpendicular upper critical field of granular Pb films near the superconductor-to-insulator transition, *Phys. Rev. B* 47 (1993) 14334.
- [40] B. Abeles, R.W. Cohen, W.R. Stowell, Critical magnetic fields of granular superconductors, *Phys. Rev. Lett.* 18 (1967) 902.
- [41] R.W. Cohen, B. Abeles, Superconductivity in granular aluminum films, *Phys. Rev.* 168 (1968) 444.
- [42] G. Deutscher, O.E. Wohlman, Critical fields of weakly coupled superconductors, *Phys. Rev. B* 17 (1978) 1249.